Published in *Contemp. Phys.* **51**, 233-248 (2010).

Contemporary Physics
Vol. 00, No. 00, July 2009, 1–23

REVIEW

Stochastic webs and quantum transport in superlattices: an introductory review

S.M. Soskin,[a,b,c*] P.V.E. McClintock,[c] T.M. Fromhold,[d] I.A. Khovanov[e] and R. Mannella[f]

[a] *Institute of Semiconductor Physics, National Academy of Sciences of Ukraine, 03028 Kiev, Ukraine*
[b] *Abdus Salam ICTP, 34100 Trieste, Italy*
[c] *Physics Department, Lancaster University, Lancaster LA1 4YB, UK*
[d] *School of Physics and Astronomy, University of Nottingham, Nottingham NG7 2RD, UK*
[e] *School of Engineering, University of Warwick, Coventry CV4 7AL, UK*
[f] *Dipartimento di Fisica, Università di Pisa, 56127 Pisa, Italy*;

(*v3.0 released 27 July 2009*)

Stochastic webs were discovered, first by Arnold for multi-dimensional Hamiltonian systems, and later by Chernikov et al. for the low-dimensional case. Generated by weak perturbations, they consist of thread-like regions of chaotic dynamics in phase space. Their importance is that, in principle, they enable transport from small energies to high energies. In this introductory review, we concentrate on low-dimensional stochastic webs and on their applications to quantum transport in semiconductor superlattices subject to electric and magnetic fields. We also describe a recently-suggested modification of the stochastic web to enhance chaotic transport through it and we discuss its possible applications to superlattices.

Keywords: stochastic webs; quantum transport; superlattices; separatrix chaos

1 Introduction

Stochastic webs exist in the phase spaces of Hamiltonian systems, that is, in the space formed by the coordinates and momenta of a dynamical system evolving in the absence of dissipation. They consist of a network of very thin thread-like regions within which the dynamics is chaotic, whereas the dynamics remains regular everywhere else. Although the concept seems abstract and mathematical at first sight, stochastic webs are now known to arise in a number of practical contexts, including for example plasma physics [1], ultra-cold atoms in optical lattices [2–4] and electrons in semiconductor superlattices (SLs) [5–11]; they have also been considered in connection with celestial mechanics [12]. The importance of the chaotic threads is that they can transport matter and energy effectively over long distances [13, 14]. In this brief and rather informal review we aim to introduce the general reader to stochastic webs, explaining what they are and discussing their recent developments and applications, taking electron transport in semiconductor SLs as our example.

We start (Section 1.1) from the definition of a Hamiltonian system, its dimensionality and integrability. Then (Section 1.2) we consider the effect of perturbations of the integrable system, which brings us to the concept of a chaotic (stochastic) layer, in particular related to resonances. The latter allows us to explain in the beginning of Section 2 the onset of the Arnold stochastic

*Corresponding author. Email: ssoskin@ictp.it

ISSN: 0010-7514 print/ISSN 1366-5812 online

DOI: 10.1080/0010751YYxxxxxxxx
http://www.informaworld.com

web in multi-dimensional systems. The main purpose of this section is to discuss the more sophisticated nature of low-dimensional stochastic webs which are, however, still related to the concept of resonance. In Section 3, we explain the limitations of the transport though the low-dimensional web and suggest a subtle way of overcoming these limitations. Finally, in Section 4, we discuss a rather unexpected application of the stochastic web concept to quantum electron transport in nanometer-scale semiconductor SLs in the presence of electric and magnetic fields. Section 5 draws conclusions.

1.1 *Hamiltonian systems*

Hamiltonian systems play an important role in physics, chemistry, biology and engineering, and form a fundamental class of dynamical systems [15–17]. They are defined by the following dynamical equations:

$$\frac{\mathrm{d}p_i}{\mathrm{d}t} = -\frac{\partial H}{\partial q_i}, \qquad \frac{\mathrm{d}q_i}{\mathrm{d}t} = \frac{\partial H}{\partial p_i}. \tag{1}$$

If the Hamiltonian H does not depend on time t, while depending only on the momenta $\vec{p} \equiv (p_1, \ldots, p_N)$ and coordinates $\vec{q} \equiv (q_1, \ldots, q_N)$, then it is called N-dimensional. If it also depends on time t, then it has the dimension $N + \frac{1}{2}$. A remarkable property of any Hamiltonian system is the equality of its full and partial derivatives with respect to time:

$$\frac{\mathrm{d}H}{\mathrm{d}t} = \frac{\partial H}{\partial t}. \tag{2}$$

In particular, for time-independent Hamiltonians, $H(\vec{p}, \vec{q})$ is conserved along the trajectory.

In general, the equations of motion (1) may not be integrable in quadratures[1] [15–17], whence the importance of *integrable* systems, i.e. those time-independent Hamiltonian systems for which a transformation $\{\vec{p}, \vec{q}\} \leftrightarrow \{\vec{I}, \vec{\theta}\}$ exists such that

$$H(\vec{p}, \vec{q}) = \tilde{H}(\vec{I}). \tag{3}$$

I_i are called actions while θ_i are called angles. It follows from (3) that $\vec{I}$ is conserved:

$$\frac{\mathrm{d}I_i}{\mathrm{d}t} = -\frac{\partial \tilde{H}}{\partial \theta_i} = 0, \tag{4}$$

while the angles θ_i change with constant speeds (for a given $\vec{I}$),

$$\frac{\mathrm{d}\theta_i}{\mathrm{d}t} = \frac{\partial \tilde{H}(\vec{I})}{\partial I_i} \equiv \omega_i(\vec{I}), \tag{5}$$

which are called frequencies.

Note that angles θ_i are cyclic variables i.e. $\vec{p}$ and $\vec{q}$ are periodic functions of θ_i with a period 2π for any θ_i [1, 15–17]. Thus, Eqs. (4) and (5) correspond to periodic or quasi-periodic motion. The simplest and most often used example of an integrable system is a one-dimensional one, which will be described in more detail below.

---

[1]When the solution of a differential equation expressible in terms of a formula involving integrations, it is said to be *solvable by quadrature.*

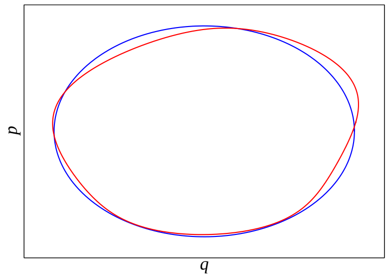

Figure 1. Schematic diagram to show a weak distortion of the majority of trajectories by a weak time-periodic perturbation: the blue line shows the trajectory of the unperturbed system, while the red line shows the stroboscopic Poincaré section of the trajectory of the perturbed one.

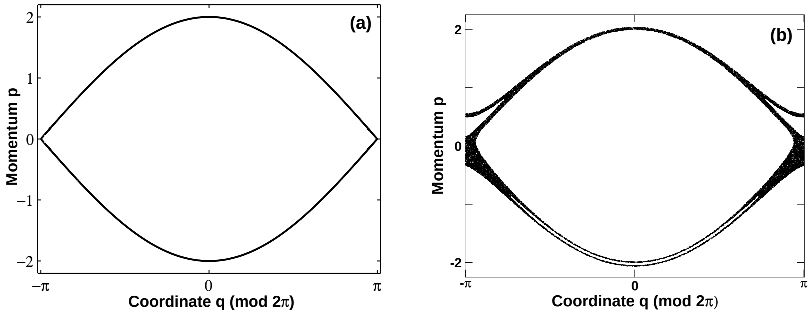

Figure 2. (a). The separatrix of the pendulum $H = H_0 \equiv p^2/2 - \cos(q)$: the separatrix corresponds to $H = H_s \equiv 1$. (b). The chaotic layer (replacing the separatrix) in Poincaré section of the ac-driven pendulum: $H = H_0 - 0.01q\cos(t)$.

1.2 *Perturbed Hamiltonian systems*

It is natural to pose the question: what is the effect of a weak perturbation on an integrable system? For the majority of cases, the answer is given by the Kolmogorov-Arnold-Moser (KAM) theory [15]: most of the trajectories are just weakly distorted by a weak perturbation while remaining regular. Let us illustrate this by an example of a one-dimensional system weakly perturbed time-periodically. In this case, it is convenient to present the trajectory in the stroboscopic *Poincaré section* [1, 15–17], i.e. presenting states of the system $\{p(t), q(t)\}$ only at the discrete sequence of instants $t = t_n \equiv t_0 + nT$ where t_0 is some initial instant, T is the perturbation period and $n = 0, 1, 2, ...$ If the trajectory is "just weakly distorted while remaining regular", then, in particular, the unperturbed trajectory and the Poincaré section of the perturbed one have the same dimension of 1 (i.e. they are just lines), and the same topology, while just slightly deviating from each other (Fig. 1).

There are, however, two kinds of situation for which KAM-theory is not valid. The first of these relates to the *separatrices* of the unperturbed systems. Let an integrable system possess a separatrix i.e. the line (or surface, or hyper-surface in the general multi-dimensional case) that separates trajectories of a different topology in the phase space[1]: e.g. in the example shown in Fig. 2(a), the separatrix separates closed trajectories (corresponding to oscillations inside the separatrix loops) from open trajectories (corresponding to the running coordinate below or above the separatrix loops). If the system is perturbed time-periodically[2], then the separatrix is replaced by a chaotic trajectory. In Poincaré section, the chaotic trajectory lies within a *chaotic layer* (Fig. 2(b)): the latter has a complicated (fractal) structure but its outer boundaries are well defined and the region delineated by these boundaries has the dimension 2, unlike the

[1]More rigorously, the separatrices may be defined as follows [18]. Let the integrable system possess a saddle i.e. a hyperbolic point in the one-dimensional case (i.e. an unstable stationary point with an exponential dynamics of trajectories approaching it), or a hyperbolic invariant torus in higher-dimensional cases. The stable (incoming) and unstable (outgoing) manifolds are called *separatrices*.

[2]In multi-dimensional cases, a time-independent perturbation also may give rise to the invalidity of the KAM-theory near the separatrix.

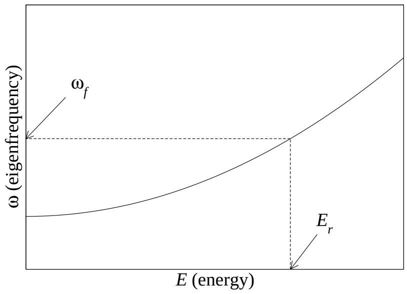

Figure 3. A schematic diagram showing the dependence of eigenfrequency ω on the energy E of an eigenoscillation, and the meaning of the resonance energy E_r.

dimension 1 of regular trajectories. Thus, even the appearance of the Poincaré section allows us to distinguish immediately between regular and chaotic trajectories, unless of course the width of the chaotic layer is less than the accuracy provided by the numerical integration of equations of motion. The theoretical prediction of the width in energy of the chaotic layer has a long and rich history. Its description on a physics level of rigour may be found in the book by Zaslavsky [17]. Studies that are more mathematically rigorous have recently been reviewed [19]. The maximum width of the layer and other significant features (high peaks) of the width as function of the perturbation frequency have recently been described [20, 21].

Another characteristic situation where the KAM-theory is invalid relates to *resonances*, i.e. to areas of the phase space where at least one of the following conditions holds

$$\begin{aligned}
&n\omega_i(\vec{I}_r) = m\omega_j(\vec{I}_r), \\
&n, m = \pm 1, \pm 2, \pm 3, \ldots, \\
&i, j = 1, 2, 3, \ldots, N, \qquad i \neq j, \\
&N = 2, 3, 4, \ldots,
\end{aligned} \tag{6}$$

or

$$\begin{aligned}
&n\omega_i(\vec{I}_r) = l\omega_f, \\
&n = \pm 1, \pm 2, \pm 3, \ldots, \\
&i = 1, 2, 3, \ldots, N - \frac{1}{2}, \\
&N = \frac{3}{2}, \frac{5}{2}, \frac{7}{2}, \ldots,
\end{aligned} \tag{7}$$

where ω_f is the frequency of the corresponding time-periodic perturbation while l is the number of the Fourier harmonic that may exist for the time-periodic perturbation (e.g. for a monochromatic perturbation, only $l = 1$ is relevant).

The rigorous treatment of motion in the resonance range is rather complicated, being related to the Poincaré-Birkhoff theorem and homoclinic and heteroclinic trajectories and tangencies [22, 23]. We do not consider it here. Rather, we give a brief interpretation of the resonance-related chaos in physical terms[1]. For the sake of clarity, consider an ac-driven 1D Hamiltonian system whose frequency of eigenoscillation ω increases monotonically with the energy of eigenoscillation $E \equiv H_0(p, q)$, while the perturbation frequency ω_f exceeds the minimum of $\omega(E)$, as shown in Fig. 3:

[1]This was given for the first time by Chirikov [24] (a clear presentation of the issues in question can be found e.g. in [17]).

$$\begin{aligned} &H = H_0(p,q) - hq\cos(\omega_f t), \qquad (8)\\ &h \ll 1,\\ &\omega_f > \omega_0 \equiv \min\{\omega(E)\}. \end{aligned}$$

Then there necessarily exists an energy E_r such that the resonance condition (7) with $n = l = 1$ holds true:

$$\omega(E_r) = \omega_f. \qquad (9)$$

Consider motion for energies close to E_r. Let us transform from variables $\{p, q\}$ to action-angle variables $\{I, \theta\}$, so that the Hamiltonian becomes

$$\begin{aligned} H(p,q) \equiv \tilde{H}(I,\theta) &= \int_{I_{\min}}^{I} \mathrm{d}\tilde{I}\omega(\tilde{I}) - h\sum_n q_n(I)\cos(n\theta)\cos(\omega_f t)\\ &\equiv \int_{I_{\min}}^{I} \mathrm{d}\tilde{I}\omega(\tilde{I}) - \frac{1}{2}hq_1\cos(\theta - \omega_f t) + ...\\ &\equiv \tilde{H}_0(I, \tilde{\theta} \equiv \theta - \omega_f t) + V_f(I, \tilde{\theta}, t), \qquad (10)\\ I(p,q) \equiv I(E) &= \frac{1}{2\pi}\oint p(q,E)\,\mathrm{d}q, \qquad E \equiv H_0(p,q),\\ \theta(p,q) &= \omega(E)\int^{q} \frac{1}{p(\tilde{q},E)}\,\mathrm{d}\tilde{q},\\ q_n \equiv q_n(I) &= \frac{1}{2\pi}\int_0^{2\pi} \mathrm{d}\theta q\cos(n\theta). \end{aligned}$$

Here, the dots "…"denote terms that vary with time much faster than the preceding term: they are denoted in the next equality as V_f. Thus, allowing for the resonance condition (9), we may introduce the slow angle $\tilde{\theta} \equiv \theta - \omega_f t$ and present the original Hamiltonian as a sum of an "autonomous"part $\tilde{H}_0(I, \tilde{\theta})$ and the time-dependent (fast-oscillating) part $V_f(I, \tilde{\theta}, t)$. It is easy to check by direct substitution into the corresponding Hamiltonian equations of motion that the dynamics of the variables I and $\tilde{\theta}$ is governed by the Hamiltonian

$$\tilde{\tilde{H}} = \tilde{H} - \omega_f I. \qquad (11)$$

Taking into account that the perturbation is small ($h \ll 1$) and, therefore, that the variation of I around the resonance value $I_r \equiv I(E_r)$ is also small, we may approximate the function $\omega(I)$ near the resonance value as

$$\begin{aligned} &\omega(I) \approx \omega_f + \omega'_r(I - I_r), \qquad (12)\\ &\omega'_r \equiv \frac{\mathrm{d}\omega}{\mathrm{d}I}\,|_{I=I_r}\ . \end{aligned}$$

From (10)-(12), we ultimately obtain the approximate auxiliary Hamiltonian governing the dynamics of $\{I, \tilde{\theta}\}$:

$$\begin{aligned}\tilde{\tilde{H}}(I,\tilde{\theta},t) &= \frac{1}{2}\omega_r'(I-I_r)^2 - \frac{1}{2}hq_1\cos(\tilde{\theta}) + V_f(I,\tilde{\theta},t) \\ &\equiv \tilde{\tilde{H}}_0(\tilde{I}\equiv I-I_r,\tilde{\theta}) + V_f. \end{aligned} \tag{13}$$

It represents the sum of a pendulum-like[1] autonomous Hamiltonian $\tilde{\tilde{H}}_0(\tilde{I},\tilde{\theta})$ and a time-periodic (fast-oscillating) part V_f that plays the role of a perturbation. The pendulum-like part $\tilde{\tilde{H}}_0$ possesses a separatrix (cf. Fig. 2(a)) while the perturbation-like part V_f tends to destroy the separatrix, replacing it with an exponentially narrow chaotic layer.

Thus we have shown that a resonance is necessarily associated with a narrow chaotic layer.

2 Stochastic webs

In the example considered above, the chaotic layer associated with the resonance provides only a narrow ($\propto \sqrt{h}$) variation of energy (or, equivalently, of action). Thus, there is no significant transport in energy. Let us pose a question: *could there be situations when a perturbation provides for chaotic transport through a large range of energies?* We now describe the three stages of conceptual evolution that led to a positive answer to this question.

2.1 *Multi-dimensional web*

First, Arnold showed in 1964 [25] through rather simple topological arguments (also presented clearly in [17]) that, if the system is multi-dimensional (namely, if $N \geq 5/2$), and if the so called non-degeneracy condition $\det(\partial^2 H/\partial I_i \partial I_j) \neq 0$ is fulfilled (in other words, if the system is sufficiently nonlinear), then resonances necessarily intersect with each other, forming an infinite *web* in the phase space along which an exponentially slow chaotic diffusion occurs.

2.2 *Low-dimensional webs*

Secondly, Chernikov et al. published an important series of papers in the late 1980s. We shall review just three of the more important of them, concentrating on the model of a harmonic oscillator subject to a plane wave, which will be relevant to our discussion of semiconductor SLs below. A good review of a broad range of the early work on low-dimensional stochastic webs may be found in [1]; more recent work is reviewed in [26] (see also [17]).

The main idea of Chernikov et al. is that a stochastic web may arise even in low-dimensional systems ($N = \frac{3}{2}; 2$) provided that the non-degeneracy condition is lifted, in other words, in this case, if

$$\frac{\mathrm{d}\omega}{\mathrm{d}I} = 0, \tag{14}$$

while the perturbation in the equation of motion is resonant and coordinate-dependent.

2.2.1 Cobweb

We now consider the best known example of a low-dimensional stochastic web, the skeleton of which in $p-q$ Poincaré section has a form resembling that of a cobweb (Figs. 4(a), 5(b)). We

[1] $\tilde{I}$ plays the role of a generalized velocity while $\tilde{\theta}$ plays the role of the generalized coordinate. Note that the generalized potential contains the small multiplier h, so that the maximal absolute value of the "velocity" $\tilde{I}$ is proportional to $\sqrt{h}$ and, therefore, is small too.

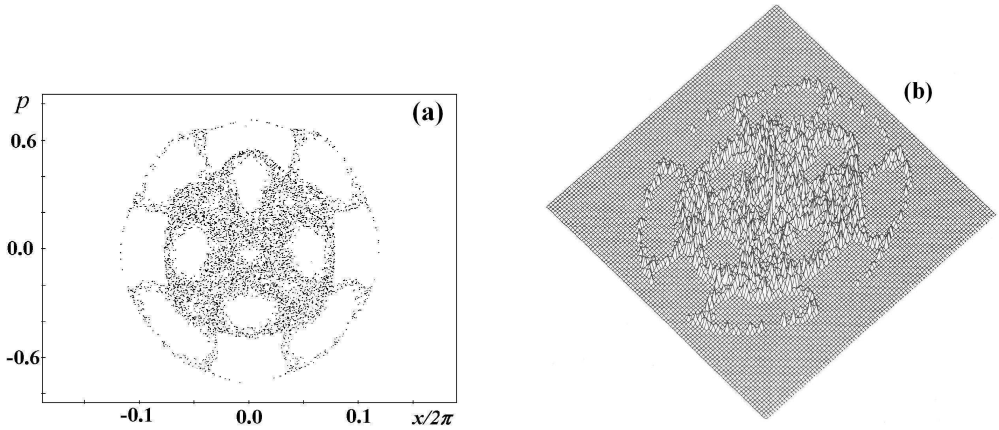

Figure 4. Stochastic web for the system (15), as obtained numerically with $\omega_0 = 1$, $\nu = 4$, $k = 15$, $\epsilon\omega_0^2/k = 0.1$ [27]. The integration time is 2×10^4 periods of oscillation $2\pi/\omega_0$. (a). Poincaré section. (b). The corresponding probability distribution.

suppose that a harmonic oscillator is perturbed[2] by a resonant plane wave [27]:

$$\begin{aligned} &\ddot{q} + \omega_0^2 q = \epsilon \frac{\omega_0^2}{k} \sin(kq - \nu t), \\ &\nu = n\omega_0, \quad n = 1, 2, 3, ... \end{aligned} \tag{15}$$

This particular model has a number of applications, especially to plasma physics [1] and to semiconductor SLs, as shown below in Sec. 4. In order to understand the origin of the stochastic web shown in Fig. 4, we

(i) transform to polar coordinates $\{\rho, \theta\}$ or, equivalently, to action-angle variables $\{I, \theta\}$:

$$\begin{aligned} &q = \rho \sin(\theta), \quad p \equiv \dot{q} = \omega_0 \rho \cos(\theta), \\ &\rho \equiv \sqrt{\frac{2I}{\omega_0}}, \end{aligned} \tag{16}$$

(ii) make use of the formula [28]

$$\cos(x \sin(\theta) - y) = \sum_{m=0}^{\infty} J_m(x) \cos(m\theta - y) \tag{17}$$

where $J_m(x)$ is a Bessel function of the mth order[1].

Using (16) and (17), it is not difficult to show that the Hamiltonian of a harmonic oscillator perturbed by a plane wave can be represented in action-angle variables as

$$H(I, \theta, t) = \omega_0 I + \epsilon \frac{\omega_0^2}{k^2} \sum_m J_m(k\rho(I)) \cos(m\theta - \nu t). \tag{18}$$

Note that, due to the resonance condition $\nu = n\omega_0$ in (15), the term in the sum in (18) corresponding to $m = n$ is nearly constant compared to other terms in the sum. So, similarly to

[2]For parameters, we use the same notation as Zaslavsky [1] and Chernikov et al. [27] while the coordinate is denoted as q (instead of x in [1, 27]: cf. Fig. 4(a)) in order to match the notation in other sections and in some figures from other works reproduced below.

[1]Note that $J_m(x)$ is an oscillatory function of x with gradually decreasing amplitude as x increases. At $x \sim 1$, the period of oscillation is $\sim 2\pi$ while the amplitude is ~ 1. For large x, the Bessel function asymptotically approaches the function $\sqrt{2/(\pi x)} \cos(x - (2m+1)\pi/4)$.

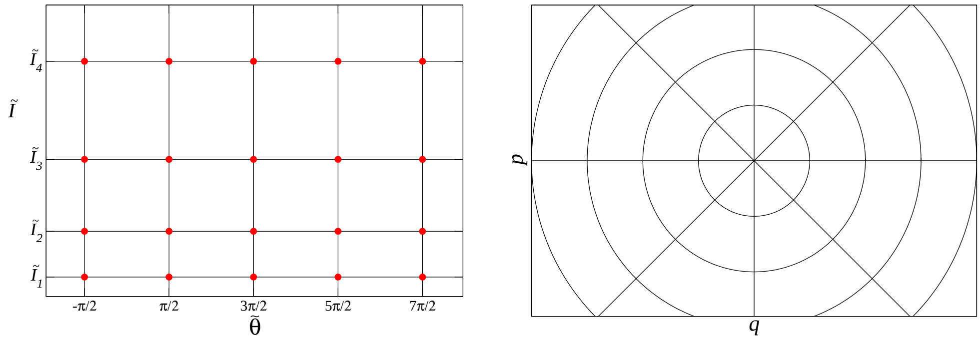

Figure 5. Left panel: schematic representation of the grid-like separatrix of the Hamiltonian $\tilde{H}_s$, as defined in Eqs. (20); saddles are shown by dots. Right panel: schematic representation of the same separatrix in Poincaré section $p - q$.

the case of nonlinear resonance considered in Section 1.2 above, it is this term that provides the major contribution to the dynamics. The other terms in the sum play the role of fast-oscillating perturbations. So we again introduce a slow variable, the angle $\tilde{\theta} \equiv n\theta - \nu t$. It is also convenient to introduce the normalized action $\tilde{I} \equiv I/n$. The dynamics of the slow variables $\{\tilde{I}, \tilde{\theta}\}$ is then governed by the auxiliary Hamiltonian $\tilde{H} \equiv nH - \nu\tilde{I}$ (as may readily be checked by direct substitution into the Hamiltonian equations of motion). Hence

$$\begin{aligned}
&\dot{\tilde{I}} = -\frac{\partial \tilde{H}}{\partial \tilde{\theta}}, \quad \dot{\tilde{\theta}} = \frac{\partial \tilde{H}}{\partial \tilde{I}}, \\
&\tilde{\theta} \equiv n\theta - \nu t, \quad \tilde{I} \equiv I/n, \\
&\tilde{H} = \tilde{H}_s + \tilde{V}_f, \\
&\tilde{H}_s \equiv \tilde{H}_s(\tilde{I}, \tilde{\theta}) = \frac{\epsilon n}{k^2}\omega_0^2 J_n(k\rho(\tilde{I}))\cos(\tilde{\theta}), \\
&\tilde{V}_f \equiv \tilde{V}_f(\tilde{I}, \tilde{\theta}, t) = \frac{\epsilon n}{k^2}\omega_0^2 \sum_{m\neq n} J_m(k\rho(I))\cos\left(\frac{m}{n}\tilde{\theta} - \left(1 - \frac{m}{n}\right)\nu t\right).
\end{aligned} \tag{19}$$

Thus, $\tilde{H}_s$ is an autonomous Hamiltonian that determines the main features of the motion of $\{\tilde{I}, \tilde{\theta}\}$, while $\tilde{V}_f$ plays the role of a fast-oscillating perturbation.

It is straightforward to show that the autonomous Hamiltonian $\tilde{H}_s$ possesses a single infinite grid-like separatrix corresponding to the zero value of $\tilde{H}_s$ (Fig. 5, left panel). The vertical filaments of the grid correspond to $\tilde{\theta}$ being equal to odd multiples of $\pi/2$ while the horizontal filaments correspond to zeros of the relevant Bessel function,

$$\begin{aligned}
&\text{separatrix}: \quad \tilde{H}_s = 0: \\
&\tilde{\theta} = (2j+1)\frac{\pi}{2}, \quad j = 0, \pm 1, \pm 2, \ldots, \\
&\tilde{I} = \tilde{I}_i, \quad i = 0, 1, 2, \ldots, \\
&J_n(k\rho(\tilde{I}_i)) = 0.
\end{aligned} \tag{20}$$

Note that the grid-like separatrix does not depend on the amplitude of the original perturbation. Rather its form is an inherent property of the harmonic oscillator driven by the resonant plane wave.

The fast-oscillating term $\tilde{V}_f$ replaces this grid-like separatrix by the narrow chaotic layer. If the separatrix (20) is represented in the Poincaré section $p - q$, it takes precisely the cobweb form shown schematically in the right-hand panel of Fig. 5. Thus we have achieved the primary goal of this subsection, to explain the onset of the cobweb-like stochastic web.

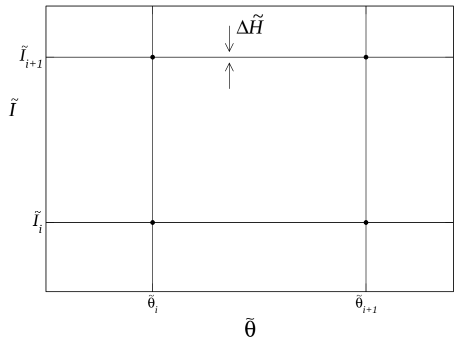

Figure 6. Schematic diagram showing the width of the chaotic layer of the web.

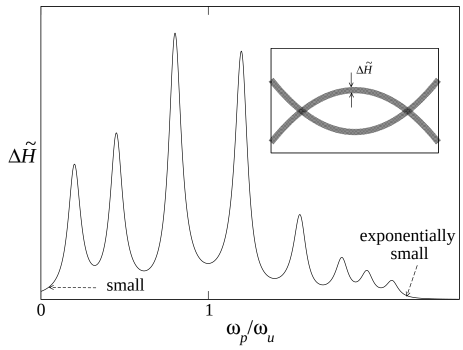

Figure 7. Typical dependence (schematic) of the width of a separatrix chaotic layer on the ratio between the frequency of perturbation and the frequency of the small-amplitude oscillation of the unperturbed system.

2.2.2 Width of the cobweb

Transport through the web is affected, not only by the shape of the web's skeleton, but also by its width, i.e. the width of the chaotic layer (Fig. 6). An exact calculation of the width is a complicated task that we will not undertake here. Rather, we will make a rough estimate sufficient to lead us to definite qualitative conclusions.

Before doing so, we make a general comment about the width in the case of a 1D system with a separatrix that is being perturbed by a time-periodic perturbation. The width depends strongly on the ratio ω_f between the frequency of the perturbation $\omega_{\text{perturbation}}$ and the frequency of small-amplitude eigenoscillations $\omega_{\text{unperturbed}}$. A schematic representation of the typical dependence is shown in Fig. 7. This figure will be discussed in more detail in Section 3. In the present context it is sufficient to emphasize that, if ω_f is large, then the width of the chaotic layer is *exponentially narrow.*

Let us now turn to the case of the web. As seen from (19), the characteristic frequency of the perturbation $\tilde{V}_f$ is $\sim \omega_0$. On the other hand, the unperturbed Hamiltonian $\tilde{H}_s$ is proportional to the small parameter ϵ. Therefore, even without a careful analysis of its oscillations, it is clear that the frequency of oscillation in any cell of its grid-like separatrix is also small. Thus, we conclude that the ratio ω_f between the perturbation frequency and the eigenfrequency is large, so that the width of the layer should be exponentially small. This conclusion is confirmed both by careful theoretical analysis and by numerical simulations [1, 27].

Moreover, the analysis of oscillations near the elliptic points inside the cells of the separatrix of $\tilde{H}_s$ shows that, for cells far from the centre, the frequency of oscillation possesses the following property[1, 27]

$$\omega_{\text{unperturbed}} \propto \frac{\epsilon}{I^{3/4}}, \tag{21}$$

i.e. it decreases as the distance from the centre increases. Conversely, the ratio ω_f increases.

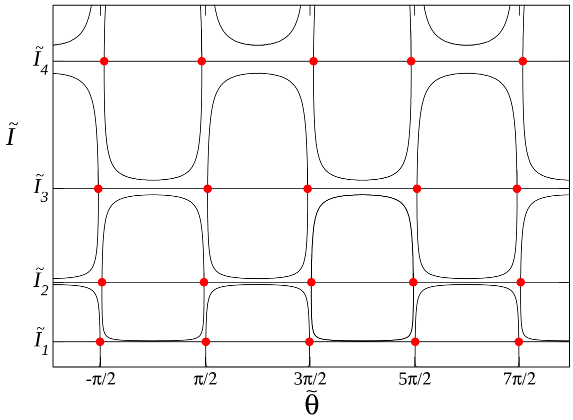

Figure 8. The separatrix for inexact resonance: the single grid-like separatrix of Fig. 5 is replaced by a set of separatrices that are distinctly separated from each other. The parameters used to compute the separatrix were: $\Delta\omega = -0.001 \neq 0$ (see Eq. (22)), $\epsilon = 0.573$ and $n = k = 1$.

This means that the width of the layer decreases exponentially quickly as the distance from the centre of the web increases. This conclusion is confirmed by Fig. 4 above: even for the moderate ϵ used in this case, the width of the layer markedly decreases as the distance from the centre grows.

2.2.3 *Inexact resonance*

Natural questions to ask in relation to the cobweb are: what happens if the oscillator differs slightly from an ideal harmonic oscillator; and what happens if the resonance is inexact? The answers were given by Chernikov et al. [29] (see also [1]). They found that the effects of anharmonicity and inexact resonance are in fact similar. So in what follows we shall, for the sake of brevity, consider only the inexactness of the resonance:

$$\nu = n\omega_0 + \Delta\omega, \quad \Delta\omega \ll \omega_0. \tag{22}$$

In this case, the autonomous resonance Hamiltonian reads as (cf. (19))

$$\tilde{H}_s = \Delta\omega\tilde{I} + \frac{\epsilon n}{k^2}\omega_0^2 J_n(k\rho(\tilde{I}))\cos(\tilde{\theta}) \tag{23}$$

As before, there are saddle points corresponding to different values of $\tilde{I}$, namely different roots of the equation $J_n(k\rho(\tilde{I})) = 0$. But this means that, unlike the resonance case ($\Delta\omega = 0$), the values of $\tilde{H}_s$ at the saddles corresponding to different $\tilde{I}$ are themselves different. This means that the single grid-like separatrix splits into infinitely many different separatrices (Fig. 8).

In order for at least two lowest separatrices to be connected, allowing chaotic transport within a unified structure (a web of a finite size, in the $p-q$ plane), the width of the chaotic layer should be more than, or of the order of, the difference in $\tilde{H}_s$ between the two lowest separatrices:

$$\Delta\tilde{H} \stackrel{\sim}{>} |\tilde{H}_s(\tilde{I}_2) - \tilde{H}_s(\tilde{I}_1)| \sim 2\pi|\Delta\omega|. \tag{24}$$

Because $\Delta\tilde{H}$ is exponentially narrow, as discussed in Section 2.2.2 above, the inequality (24) means that the stochastic web may be formed only if the perturbation frequency lies in an *exponentially small vicinity* of the resonance.

2.2.4 *Uniform web*

As already demonstrated above, the cobweb cannot in practice provide transport to arbitrarily large energies because of the exponentially fast decrease in the width of the chaotic layer with distance from the centre of the web. This limitation is overcome in another type of the stochastic

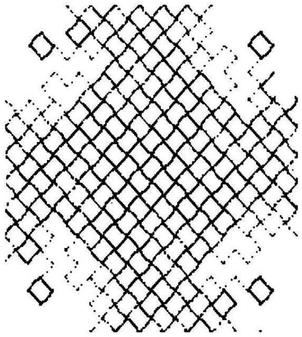

Figure 9. Example of a uniform web in $p-q$ Poincaré section [1].

web, called the *uniform web* [30] (see also [1]). Here, instead of being perturbed by a plane wave, the harmonic oscillator is perturbed by short kicks that are periodic in space and time such that the kick frequency is equal to the eigenfrequency of the oscillator or to one of its multiples:

$$\ddot{q} + q = -\epsilon \sin(kq) \sum_{n=-\infty}^{\infty} \delta(t - nT), \tag{25}$$

$$T = \frac{2\pi}{\nu}, \quad \nu = 1, 2, 3, \ldots$$

The web then covers the whole phase space uniformly, as shown in Fig. 9.

We note however that the width of the chaotic layer is still exponentially small if the amplitude of the perturbation is small [1, 29].

3 Modified stochastic webs

It is clear from the above discussion that a serious limitation affecting transport through any chaotic web is the exponential narrowness of the web's chaotic layer, which leads to exponentially slow transport. Soskin et al. [21, 31, 32] recently suggested a way of overcoming this problem by making a subtle modification of the webs leading, in turn, to exponential growth in the width of the chaotic layer. We shall demonstrate this idea on our example of the cobweb, both because it is relevant to the application to the semiconductor SLs and because, in this case, it also leads to a dramatic increase in the size of the web.

3.1 *Exact resonance case*

We have found that there is an inherent limitation in the size of the cobweb. It does not relate to the inevitably finite time of numerical simulations, which places a practical limit on the distance over which the transport can be followed, but is characteristic of the cobweb itself. Our numerical simulations show (Fig. 10) that, for the given parameters, the inner two-and-a-half loops of the web are distinctly *separated* from the adjacent outer one-and-a-half loops by regular trajectories. This might possibly be accounted for theoretically by consideration of higher-order approximations of the averaging method [33]. We may speculate that such an approach could show that, instead of a single infinite cobweb skeleton, there are many separate separatrices (of the one-and-a-half loop shape) lying closely together, but that they might then coalesce due to the chaotic layers dressing them as a result of the perturbation. Because the width of the layer decreases exponentially fast with increasing distance from the centre, this would mean that coalescence would occur only within a few inner loops. Just this is observed in Fig. 10, even despite that ϵ is moderate rather than small.

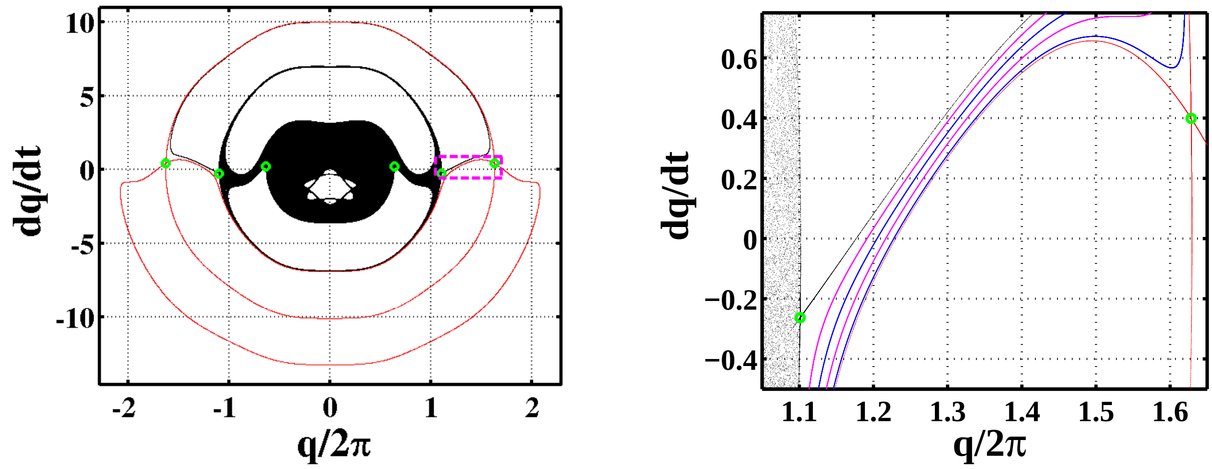

Figure 10. Left figure. Poincaré section for the system $\ddot{q} + q = \cos(q - t)$. The saddles (marked by green circles) have been found numerically. Four inner saddles belong to one and the same chaotic trajectory (shown in black) which forms two-and-a-half inner loops of the stochastic web. Two remaining (outer) saddles generate another (shown in red) chaotic trajectory which covers a very thin chaotic layer and is distinctly separated from the black chaotic trajectory. Right figure. The area within the dashed magenta rectangle of the left figure is shown on a larger scale. Apart from the black and red chaotic trajectories, we show (in magenta and blue) examples of regular trajectories (corresponding to invariant tori) lying in between the chaotic trajectories.

One may reasonably ask: *Is there any subtle way to substantially increase the size of the web and to enhance transport through it?*

In order to answer this question, let us recall the reason for the exponential narrowness of the chaotic layer. It follows from Fig. 7 that it is attributable to the frequency of the perturbation $\tilde{V}_f$ being much higher than the eigenfrequency of the unperturbed resonant Hamiltonian $\tilde{H}_s$. It is clear from Fig. 7 that the width of the layer would be much larger if we could manage to modify the original system in such a way that a new perturbation of the resonance Hamiltonian had a component whose frequency was of the order of, or less than, the eigenfrequency of the resonance Hamiltonian $\tilde{H}_s$. In fact, this may readily be accomplished in at least two different ways: (i) one can *add* to the original plane wave a small perturbation of the slightly shifted frequency (it can itself be e.g. a plane wave); (ii) one can modulate weakly the *angle* of the original plane wave at a low frequency. We demonstrate below only the second option (it will be especially convenient for realization of the phenomena in SLs, as shown in Section 4 below).

We therefore consider the modified system (cf. the original Eq. (15)):

$$\begin{aligned}
&\ddot{q} + \omega_0^2 q = \epsilon\frac{\omega_0^2}{k}\sin(kq - \nu t - h\sin(\Omega t)), \qquad (26)\\
&\nu = n\omega_0, \quad n = 1, 2, 3, ...,\\
&h \ll 1, \quad \Omega \stackrel{\sim}{<} \omega_{\text{unperturbed}} \sim \frac{\epsilon\omega_0}{I^{3/4}}.
\end{aligned}$$

Of course, the latter inequality cannot be satisfied for an arbitrarily large I, but it can be true for a sufficiently high value of I which greatly exceeds the original cobweb size in terms of I.

Repeating the same procedure used above in the derivation of Eq. (19), i.e. transforming to action-angle variables, introducing the slow angle $\tilde{\theta}$ and the auxiliary Hamiltonian $\tilde{H} \equiv nH - \nu\tilde{I}$ which governs the dynamics of $\{\tilde{I} - \tilde{\theta}\}$, we can derive:

$$\begin{aligned}
&\tilde{H} = \tilde{H}_s^{(\text{modified})} + \tilde{V}_f, \qquad (27)\\
&\tilde{H}_s^{(\text{modified})} \approx \tilde{H}_s + h\frac{\epsilon n}{k^2}\omega_0^2 J_n(k\rho(\tilde{I}))\sin(\tilde{\theta})\sin(\Omega t)
\end{aligned}$$

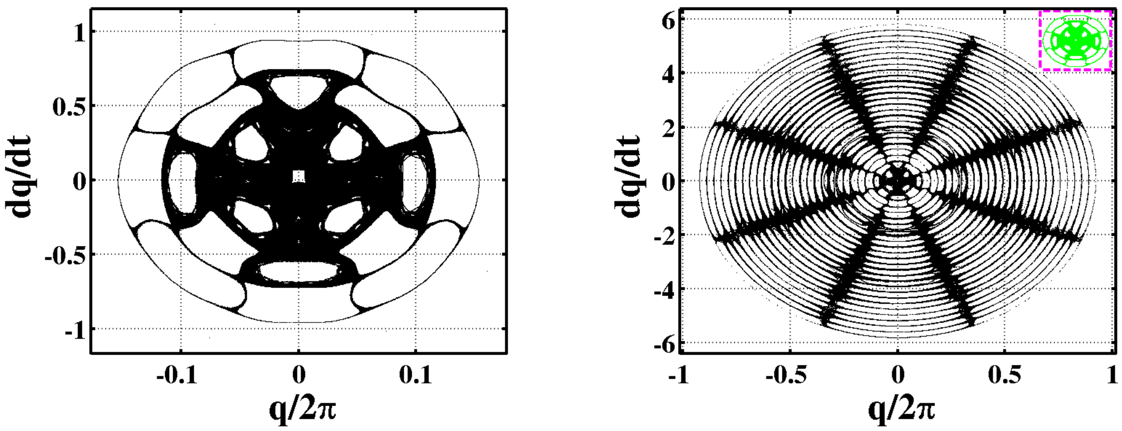

Figure 11. Poincaré section for a trajectory of the system (28) with initial state $q = 0.1$, $\dot{q} = 0$ (at instants $t_n = nT$ where $T \equiv 2\pi/0.02$ is the period of the modulation and $n = 1, 2, 3, ...600000$) for $h = 0$ (left panel) and $h = 0.1$ (right panel). A symplectic integration scheme of the fourth order is used, with an integration step $t_{int} = \frac{2\pi}{40000} \approx 1.57 \times 10^{-4}$, so that the inaccuracy at each step is of the order of $t_{int}^5 \approx \times 10^{-19}$. The left panel corresponds to the conventional case considered in [1, 17, 27]. The right panel demonstrates that the modulation, although weak, greatly enlarges the web size (note the different axes scales), thereby greatly enhancing the chaotic transport. The inset in the top right hand-corner plots the left-hand panel on the same scale, thereby illustrating the dramatic extent of this enlargement.

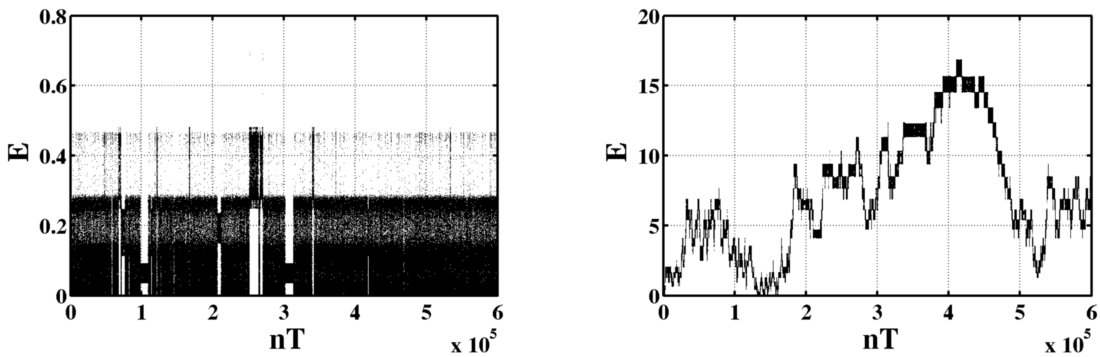

Figure 12. Dynamics of the energy for the same systems as in Fig. 11.

(in the derivation, we took into account in particular the smallness of h).

Unlike the original autonomous slow resonance Hamiltonian $\tilde{H}_s \equiv \tilde{H}_s(\tilde{I}, \tilde{\theta})$, the modified slow part of the Hamiltonian, i.e. $\tilde{H}_s^{(\text{modified})}$, depends on time: it contains a term $\propto h$ which oscillates at a low frequency Ω. It is this slowly oscillating additional term (rather than the former fast-oscillating perturbation term $\tilde{V}_f$) that now determines the width of the layer: the width is moderately small (due to the smallness of h and ϵ), rather than exponentially small as in the original setup. This exponential growth in the width of the layer gives rise to substantial growth in the size of the cobweb.

To illustrate the above ideas, we use the following example:

$$\ddot{q} + q = 0.1\,\sin[15q - 4t - h\sin(0.02\,t)]. \tag{28}$$

For $h = 0$, this coincides with the conventional cobweb example developed in [1, 17, 27].

Comparison of the left and right panels of Fig. 11, corresponding to $h = 0$ and $h = 0.1$ respectively, reveals a 6-fold increase in the size of the web in terms of q and $p \equiv \mathrm{d}q/\mathrm{d}t$:

$$n_{q,p} \approx 6. \tag{29}$$

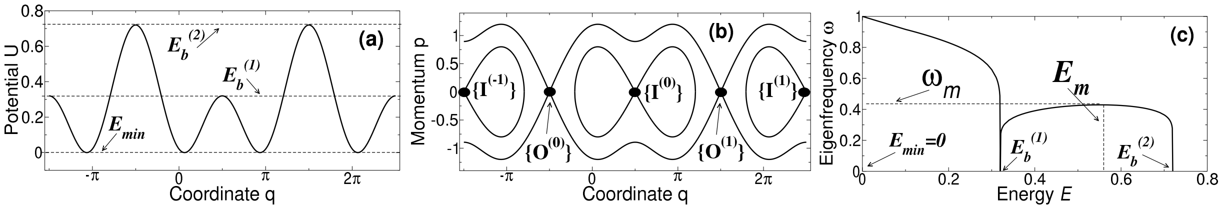

Figure 13. (a) The potential $U(q) = (0.2 - \sin(q))^2/2$, (b) the separatrices in the phase space, and (c) the frequency of oscillation as a function of energy $\omega(E)$ for the autonomous potential system $H_0(p,q,) = p^2/2 + U(q)$.

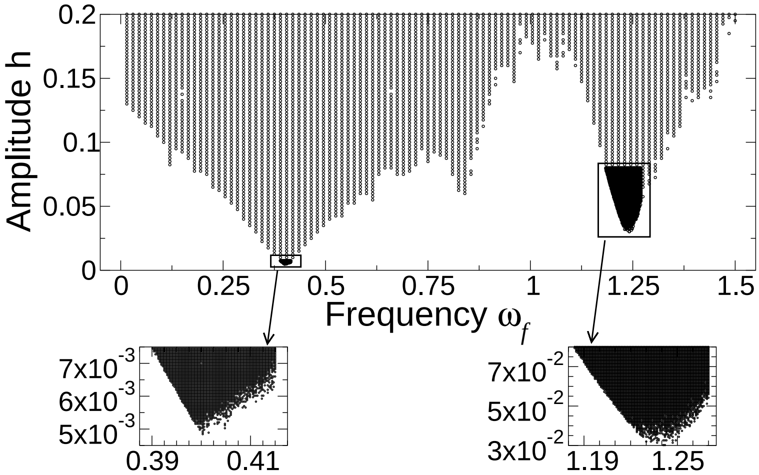

Figure 14. The bifurcation diagram in the plane of amplitude and frequency of perturbation for the system $H = H_0 + hq\cos(\omega_f t)$ with H_0 as in Fig. 13. The area of $\{h, \omega_f\}$ for which there is a global chaos between the separatrices is shaded. The lower boundary of the shaded area therefore corresponds to the onset of global chaos, representing the function $h_{cr}(\omega_f)$.

We emphasize that the modulation giving rise to this substantial increase is actually very small: its amplitude of 0.1 is about 60 times smaller than 2π which is the relevant scale for the angle.

The corresponding increase of the size in terms of energy is proportional to the square of $n_{q,p}$:

$$n_E = n_{q,p}^2 \approx 36. \tag{30}$$

Fig. 12 shows this explicitly and, in addition, demonstrates that the mode of transport is significantly changed.

3.2 *Inexact resonance*

Our idea of an additional small modulation of the angle of the plane wave is equally fruitful in the case of an inexact resonance. The frequency band (around the resonance) in which the web-like structure is formed may grow exponentially: instead of the exponentially narrow band found in the absence of modulation, we may have a moderately narrow band.

Moreover, there is a nontrivial spectral dependence of this growth: it reflects a universal mechanism for facilitation of the onset of chaos between adjacent separatrices, discovered recently by Soskin, Mannella and Yevtushenko [34]. To explain this mechanism, we use their example: it is a potential system with a spatially periodic potential possessing two barriers of different height within one period (Fig. 13(a)). Naturally, there are two kinds of separatrices (Fig. 13(b)). It was shown [34] that the frequency of oscillation ω as a function of energy E possesses a local maximum ω_m between the separatrices and, moreover, ω is close to ω_m over most of the inter-separatrix energy range (Fig. 13(c)). The latter property is valid for any system with two or more separatrices and is particularly important in the present context.

If we perturb the system with a time-periodic perturbation of frequency slightly lower than ω_m then, due to the flatness of $\omega(E)$ over most of the inter-separatrix range of E, two nonlinear

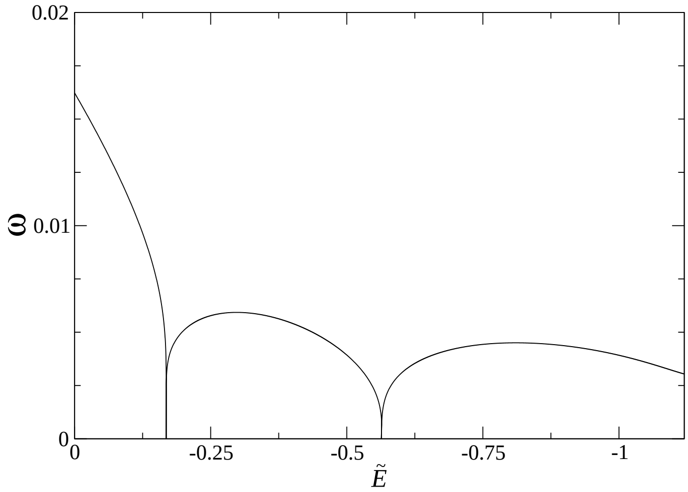

Figure 15. Frequency of oscillation in the autonomous Hamiltonian system (23) with parameters as in (31), as a function of the corresponding energy $\tilde{E} \equiv \tilde{H}_s$.

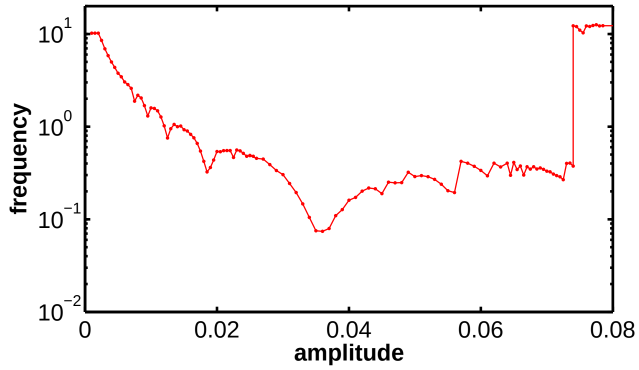

Figure 16. The spectral dependence (i.e. dependence on Ω) of the critical amplitude h of the modulation required for initial web formation i.e. for chaotic connection of the first two separatrices of $\tilde{H}_s$ (23) to occur. Note the logarithmic vertical scale.

resonances arise that are very wide in terms of energy. Even a rather small amplitude of perturbation may be sufficient for these nonlinear resonances to overlap with each other and with the separatrix chaotic layers, thus connecting the latter by the chaotic transport. This has been confirmed both theoretically and in numerical simulations. Consequently, a critical perturbation amplitude h_{cr} is required for chaotic transport between the separatrix chaotic layers (which may be considered as the onset of global chaos between them). As a function of the perturbation frequency ω_f, it possesses a deep minimum[1] at a frequency approximately equal to ω_m. This is not only seen in the simulations (Fig. 14) but is also well described by the theory [34].

The situation is similar for modulation-assisted formation of the web in the case of inexact resonance between the plane wave frequency and that of the oscillator. To demonstrate this, we use the following example (the parameters correspond to those used in experiments on semiconductor SLs):

$$\ddot{q} + q = \epsilon \sin[q - \nu t - h \sin(\Omega t)], \qquad (31)$$
$$\nu = 1.02292, \quad \epsilon = 0.573.$$

For $h = 0$, a stochastic web is not formed because the $\Delta\omega \equiv \nu - 1 \approx 0.023$ is too large for the

[1]If the perturbation is parametric rather than additive, then the deepest minimum may occur at some multiple of ω_m rather than at ω_m itself [34].

chaotic connection of any separatrices of $\tilde{H}_s$ (23) to occur. We have calculated numerically the two lowest separatrices in the plane $\tilde{I} - \tilde{\theta}$ (cf. Fig. 8), and then obtained the frequency ω of oscillation of $\tilde{I}$ (or, equivalently, of the shift by 2π of $\tilde{\theta}$) as a function of the auxiliary energy $\tilde{E} \equiv \tilde{H}_s$: see Fig. 15. There is a local maximum that is clearly similar to that in Fig. 13(c).

Then we switch on the modulation of the wave angle and, for each given Ω, increase h gradually, until the web is formed i.e. until chaotic connection occurs between the first two separatrices $\tilde{H}_s$. This may be considered as the formation of the web. The spectral dependence of the corresponding critical amplitude is shown in Fig. 16. Similar to Fig. 14, it exhibits a deep minimum (note the logarithmic scale) at a frequency which is a little smaller than the local maximum of the dependence $\omega(\tilde{E})$: cf. Fig. 16.

4 Semiconductor superlattices in electric and magnetic fields

An application of the stochastic cobweb in nanoscience was recently identified and discussed in a series of publications by researchers from the University of Nottingham [5–8, 10]. They considered quantum electron transport in nanometre-scale 1D semiconductor SLs subject to a constant electric field along the SL axis and to a constant magnetic field (Fig. 17(a,b)). The spatial periodicity of the SL layers gives rise to minibands for the electrons (Fig. 17(c)). In the tight-binding approximation, the electron's energy E as a function of its momentum $\vec{p}$ in the lowest miniband is given by [5, 8]

$$E(\vec{p}) = \frac{\Delta[1 - \cos(p_x d/\hbar)]}{2} + \frac{p_y^2 + p_z^2}{2m^*}, \tag{32}$$

where x is oriented along the SL axis, Δ is the miniband width, d is the SL period, and m^* is the electron effective mass for motion in the transverse (i.e. y-z) direction.

Thus, the quasi-classical motion of an electron of charge e in an electric field $\vec{F}$ and a magnetic field $\vec{B}$ can be described by:

$$\frac{\mathrm{d}\vec{p}}{\mathrm{d}t} = -e\{\vec{F} + [\nabla_{\vec{p}} E(\vec{p}) \times \vec{B}]\}. \tag{33}$$

It was shown in [5] that, for a constant electric field along the SL axis $\vec{F} = (-F, 0, 0)$ and constant magnetic field with a given angle θ to the axis $\vec{B} = (B\cos(\theta), 0, B\sin(\theta))$, the dynamics of the z-component of momentum p_z reduces to the equation of motion of an auxiliary harmonic oscillator subject to a plane wave i.e. to the equation considered in the previous sections[1,2]:

$$\ddot{p_z} + \omega_0^2 p_z = \epsilon \frac{\omega_0^2}{k} \sin(kp_z - \nu t + \phi), \tag{34}$$
$$\omega_0 = \omega_c \cos(\theta), \quad \omega_c \equiv \frac{Be}{m^*},$$
$$\nu = \omega_B, \quad \omega_B \equiv \frac{eFd}{\hbar},$$
$$\epsilon = \frac{\Delta m^* d^2 \tan^2(\theta)}{\hbar^2},$$
$$k = \frac{d\tan(\theta)}{\hbar},$$
$$\phi = \pi + \frac{d}{\hbar}[p_x(t=0) + p_z(t=0)\tan(\theta)].$$

We emphasize that, despite its classical appearance, Eq. (34) has an inherently quantum origin: most of the parameters contain Planck's constant $\hbar$.

The dynamics of the system is fully determined by the dynamics of p_z. Fig. 18 shows how the trajectory of an electron in the x-z plane changes with the angle of the magnetic field.

At $\theta = 0$, the plane wave has zero amplitude and the motion along the x- and z-directions is separable. Electrons undergo Bloch oscillations along x (due to the presence of the constant electric field) and cyclotron motion about $\vec{B}$ (Fig. 18(a)). The motion is localized.

Tilting $\vec{B}$ produces nonlinear coupling of the Bloch and cyclotron motion: as $\theta \neq 0$, the plane wave in (34) acquires a non-zero amplitude. This causes some moderate delocalization of trajectories (Fig. 18(b)). The delocalization grows very fast (Fig. 18(c)) when θ reaches values corresponding to the integer values $r \equiv \omega_B/(\omega_c \cos(\theta))$, in other words to the resonance $\nu = n\omega_0$. This strong delocalization in x is a consequence of the onset of the stochastic web for the motion of p_z (34).

It is remarkable that the quantum probability density $|\Psi(x,z)|^2$, calculated by solution of the Schrödinger equation in the SL model potential subjected to electric and magnetic fields should so nicely follow quasi-classical trajectories based on the dynamics of p_z (34): see Fig. 18.

As shown in [5, 6], the delocalization of the electrons[1] strongly affects their drift velocity v_d and, as a consequence, the current I and the current-voltage dependence $I(V)$. There are clear manifestations of the resonances, both in the theoretical curves $v_d(F)$, $I(V)$, $\mathrm{d}I/\mathrm{d}V$ (see Fig. 17(d), Fig. 19(c) and Fig. 19(d) respectively), and in the experimental curves $I(V)$ and $\mathrm{d}I/\mathrm{d}V$ (Figs. 19(a) and (b) respectively). Thus there is clear evidence for stochastic web formation in quantum electron transport, providing the basis for a conceptually new method for its control. When scattering is included *a priori* in the semiclassical equations of motion, the stochastic web, and stable islands that it enmeshes, evolve into limit cycles. These limit cycles also exhibit sharp resonant delocalization and their locations in phase space closely reflect the underlying web topology [8].

Finally, we pose a question: could the modification of the stochastic web discussed in the previous section be of use for the SLs? Its seems [21, 31, 32] that this is indeed the case. As shown in Section 3 above, modulation of the wave angle results in a large increase of the web size. It was noted in [5] that the delocalization in x is proportional to the web size in terms of the energy of the oscillator in p_z, i.e. to $E = \dot{p_z}^2/2 + \omega_0^2 p_z^2/2$ (cf. Fig. 18). The only question is

[1]The only small difference is the presence of a constant shift ϕ in the wave angle, but it is inessential.
[2]The motion of electrons in a biased SL with a tilted magnetic field can also be linked to the ultra-fast Fiske effect observed for a Josephson junction coupled to an electromagnetic resonator [35].
[1]Seemingly paradoxically, one must take account of scattering in the calculation: if the motion were purely Hamiltonian, the position of the electron averaged over time would be constant.

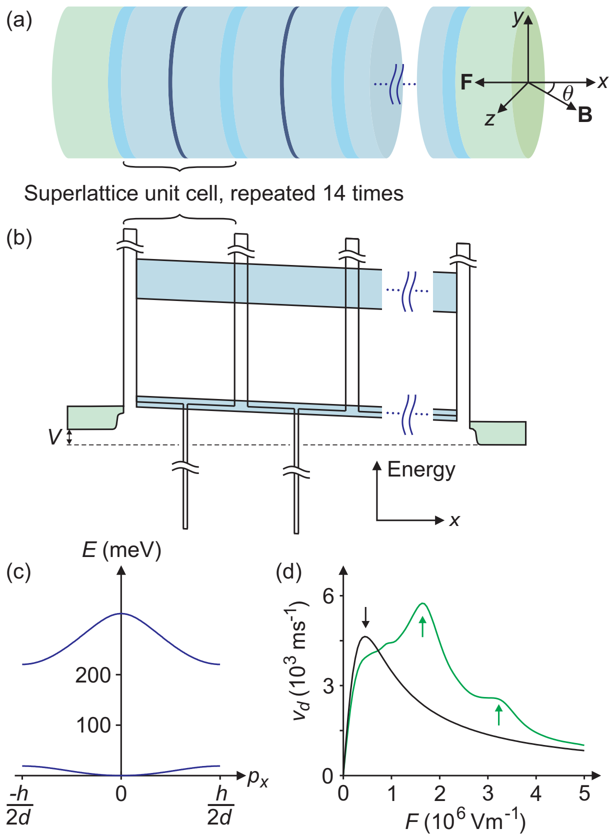

Figure 17. (a). Schematic diagram of the SL. Its unit cell comprises two 3.5-nm-thick Ga-As layers (light blue), a 0.3-nm-thick InAs layer (dark blue), and a 1-nm-thick AlAs barrier layer (mid blue). The structure contains 14 unit cells, enclosed by 50-nm-thick GaAs ohmic contacts (green). (b). Schematic variation of the electronic potential energy with position x normal to the layers, for $V \neq 0$. The quantum wells produce a periodic potential (only two complete unit cells are shown for clarity supporting two minibands (blue)). Green areas represent electron gases in the contacts. (c). Energy versus crystal momentum dispersion curves for the two minibands. (d). Plots of the drift velocity v_d versus F calculated for $B = 11$T with $\theta = 0$ (black curve: arrow marks peak) and $\theta = 45°$ (green curve: arrows mark additional peaks). Reprinted by permission from Macmillan Publishers Ltd: [Nature] [6], copyright (2004).

how the SL should be perturbed in order for the modulation term to appear in the dynamical equation for p_z. One suggestion [21, 31, 32] is that, in a manner similar to the derivation of Eq. (34), one can show that the modulation term in the equation for p_z appears if an ac-component is added to the constant electric field:

$$F \rightarrow F + F_{ac} \cos(\omega_{ac} t). \tag{35}$$

Then, the following modulation term is added in the wave angle in Eq. (34):

$$h \sin(\omega_{ac} t), \qquad h = \frac{F_{ac}}{F} \frac{\omega_B}{\omega_{ac}}. \tag{36}$$

To compare the resulting equation with the example (28) that we studied numerically, we transform to normalized time

$$t \rightarrow \tilde{t} \equiv \omega_0 t. \tag{37}$$

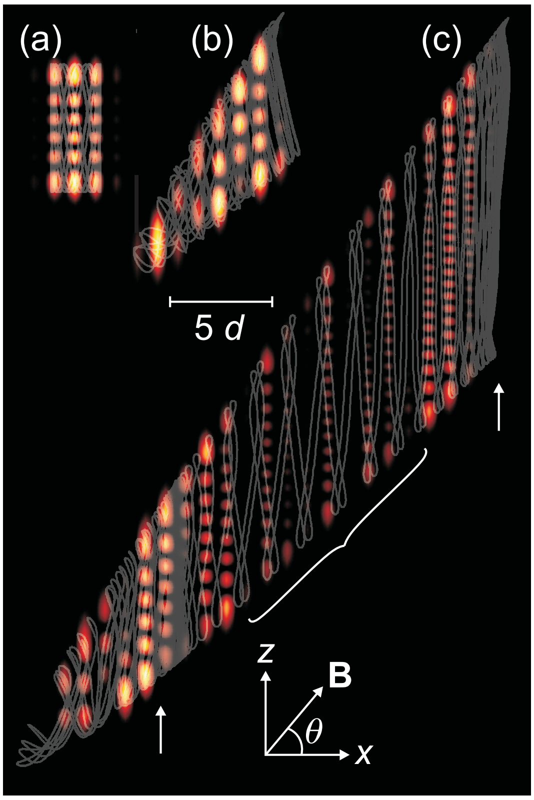

Figure 18. Electron trajectories and wavefunctions. Grey translucent curves: classical electron trajectories in the x-z plane (axes inset) overlaid on corresponding plots of $|\Psi(x,z)|^2$ (black zero, yellow high) at $B = 11$T. (a). When $\theta = 0$, the probability distribution is concentrated within the turning points of the classical trajectory. (b). Off resonance, here for $r = (1+\sqrt{5})/4)$ and $\theta = 50°$, the trajectories and wave functions extend a little but are still quite localized. (c). On resonance, here for $r = 1$ and $\theta = 50°$, the wave functions extend across many SL periods, in correspondence with the extended classical trajectories. A region of high probability density (yellow peaks) associated with a concentration of orbital loops, occurs when the electron is trapped on the first (inner) ring-shaped filament of the web (lower left-hand arrow marks the x value corresponding to this ring) and is therefore unable to progress through the SL. But when the electron transfers onto the quasi-linear filaments, it shifts rapidly along x, following widely spaced orbital loops (within bracket), which correspond to low probability density. The wavefunction is bounded from the right by the second ring-shaped web filament (right-hand arrow marks x position corresponding to this ring), which impedes electron flow. Reprinted by permission from Macmillan Publishers Ltd: [Nature] [6], copyright (2004).

Then the equation of motion for p_z is:

$$\frac{\mathrm{d}^2 p_z}{\mathrm{d}\tilde{t}^2} + p_z = \frac{\epsilon}{k}\sin(kp_z - \nu\tilde{t} + \phi + h\sin(\Omega\tilde{t})), \tag{38}$$

$$\Omega = \frac{\omega_{ac}}{\omega_0}, \qquad h = \frac{F_{ac}}{F}\frac{\nu/\omega_0}{\Omega},$$

where all other parameters are as in Eq. (34).

Thus, if the parameters are similar to those in (28), in particular: $h = 0.1$, $\Omega = 0.02$, $\nu/\omega_0 = 4$, then we will have an enlargement in E as found for Eq. (28): $n_E \approx 36$. In order to achieve this, we need $F_{ac}/F = h\Omega/(\nu/\omega_0) = 1/2000$. This means that in order to achieve delocalization of the electron by a factor of about 40, we need to add to the constant electric field an ac-component of amplitude that is smaller than the constant component by a factor of 2000! We remind the reader that the reason for such a dramatic change when an ac-component is added is the exponentially strong enhancement of chaotic transport through the stochastic web due to the modulation of the wave angle.

Recently, the effects of stochastic web formation on the high-frequency (GHz-THz) performance of the SLs has been considered [10, 11]. Modulation of the $v_d(F)$ curves, induced by stochastic web formation, leads to the formation of multiple propagating electron accumulation

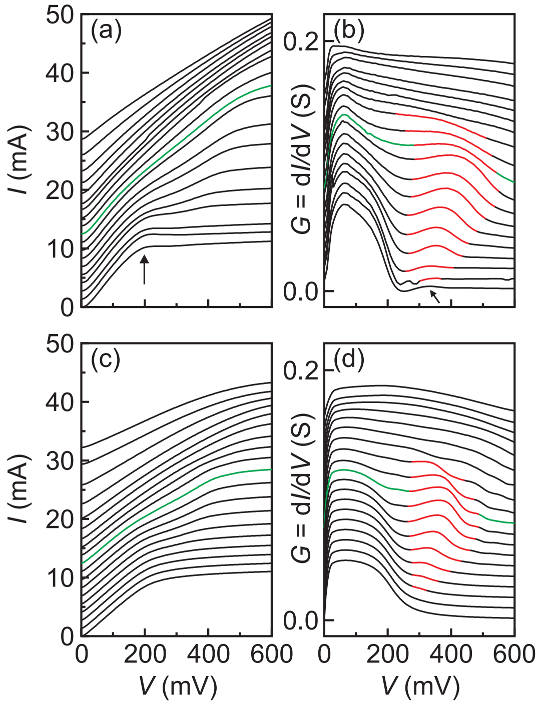

Figure 19. Resonant enhancement of current. (a). Experimental $I(V)$ curves measured for $B = 11$T and $\theta = 0$ (bottom curve) to 90° (top curve) at 5° intervals at a lattice temperature of 4.2K. For $10° \leq \theta \leq 55°$, each curve contains a region of enhanced I beyond $V \approx 250$mV. (b) Differential conductance plots of the data in (a) reveal strong resonant peaks (red). (c). Theoretical $I(V)$ characteristics (for same parameters as in (a)). (d). Differential conductance plots of the traces in (c). Curves in (a)-(d) are offset vertically for clarity and those for $\theta = 45°$ are green. In theory and experiment, the resonant peaks in $G(V)$ initially shift slightly to higher V as θ increases, because the enhanced conductance leads to higher electron charge density in the SL, which increases F and V. Reprinted by permission from Macmillan Publishers Ltd: [Nature] [6], copyright (2004).

and depletion regions (charge domains), which greatly increase both the strength and frequency of the associated temporal current oscillations. Chaos-assisted motion through stochastic webs may, therefore, provide a mechanism for controlling the collective dynamics of electrons in SLs and, hence, for enhancing their THz performance by using *single-particle* miniband transport to tailor the shape of the $v_d(F)$ curves.

5 Conclusions

We have shown that, in general, there is a possibility for energy in a Hamiltonian system to be increased from small to rather large values as a result of transport through a stochastic web.

In a multi-dimensional system, the onset of a stochastic web is a common phenomenon, predicted by Arnold in 1964. In the present review, we have been more interested in the low-dimensional stochastic webs discovered by Chernikov et al. in the late 1980s. They occur in special situations: in a harmonic, or nearly harmonic, oscillator driven by perturbations periodic in time and space that are resonant, or nearly resonant, with the oscillator.

We emphasized that the stochastic cobweb can arise when the oscillator is driven by a weak resonant, or nearly resonant, plane wave. The exponentially small width of a strand of the web is a characteristic feature of all stochastic webs and it decreases exponentially fast as the distance from the centre of the cobweb increases. Moreover there is an inherent limitation on the size of the cobweb. Soskin et al. have suggested how to overcome the restriction in size of the cobweb and the exponential narrowness of its chaotic layer, just by slightly modifying the system by means of a small slow modulation of the angle of the plane wave.

The model of the stochastic web turned out to be directly relevant to the quantum transport of electrons in semiconductor SLs in constant electric and magnetic fields, as demonstrated by

Fromhold et al.: the quantum transport dynamics reduces to the model of the harmonic oscillator perturbed by a plane wave, where parameters are determined by the values of the electric and magnetic fields, by the angle between them, by the period of the SL, by the charge and the effective mass of the electron, and by Planck's constant. At certain values of the parameters, in particular of the electric field, resonance occurs between the oscillator and the plane wave, resulting in the onset of the stochastic cobweb and, consequently, in a strong delocalization of the electron which, in turn, increases the current and gives rise to a peak in the dependence of the differential conductivity on voltage.

An addition to the constant electric field of a small slow ac-component results in the slow modulation of the plane angle and, therefore, promises to strongly increase the delocalization of the electron and to enhance a range of related phenomena.

Acknowledgements

The authors gratefully acknowledge financial support from the Royal Society of London, the International Centre for Theoretical Physics (Trieste), Pisa University and the Engineering and Physical Sciences Research Council (UK). PVEMcC acknowledges the hospitality of the Institute of Semiconductor Physics during his visit to Kiev, during which the review was conceived. SMS acknowledges the hospitality of Lancaster University, where work relevant to some parts of the review was carried out, the hospitality of the University of Nottingham, where he discussed relevant issues during his visit, and the hospitality of Pisa University, where the first draft of the review was prepared.

Notes on contributors

Stanislav M. Soskin graduated from Kiev State University in 1982 and obtained PhD from the Institute of Semiconductor Physics (Kiev, Ukraine) in 1988. At present, he is a Leading Scientific Researcher in the Theoretical Physics Department of the Institute of Semiconductor Physics. He is also an Associate Member of the International Centre for Theoretical Physics (Trieste, Italy) and a visiting member of the Physics Department in Lancaster University. He is an author of about 80 papers, including a number of reviews, mainly in the areas of fluctuation phenomena and nonlinear dynamics.

Peter V.E. McClintock is Professor of Physics at Lancaster University. After his education at Queen's University Belfast and Oxford University, followed by postdoctoral research at Duke University, he came to Lancaster in 1968. He was a SERC/EPSRC Senior Fellow, 1990-1995. His research interests include low temperature physics, superfluidity, quantum turbulence, nonlinear dynamics and, most recently, the applications of nonlinear dynamics to biomedical problems.

T. Mark Fromhold was born in 1965 in York, England. He was awarded a first-class honours degree in physics from the University of Durham (1986) and a PhD in condensed matter theory from the University of Nottingham (1990). He worked as a post-doctoral research assistant at the University of Warwick and as a medical physicist at Lincoln County Hospital (1991). He was a visiting scientist at the National Research Council (NRC) Ottawa (1995/1996) and held a Gordon Godfrey Fellowship at the University of New South Wales (1996). In 1995, he was awarded a 5 year EPSRC Advanced Fellowship. At the end of this Fellowship, he became a Lecturer in Physics at the University of Nottingham and was promoted to Reader in Theoretical Physics (2001) and Professor of Physics (2004). His research interests include quantum transport and chaos in semiconductor heterostructures, ultracold atoms, and atom chips.

Igor A. Khovanov is an EPSRC Advanced Fellow and Lecturer in the School of Engineering in the University of Warwick. Following his undergraduate education, PhD, and academic position at Saratov State University he was a Humboldt Research Fellow in the Humboldt University in Berlin, and then EPSRC Advanced Fellow in Lancaster before moving to his permanent position in Warwick. His research interests include nonlinear dynamics and fluctuation theory and their applications to engineering and biomedical problems ranging from the stress dynamics of dilute alloys to the modelling of biological ion channels.

Riccardo Mannella was born in Italy in 1960. After completing his Laurea degree in Pisa, and a PhD in Lancaster, he was a postdoctoral research associate both in Lancaster and in Pisa. From 1992 he was a Physics Researcher in Pisa University, and in 2005 he was appointed to his present position as Professor of Physics in the Veterinary Faculty of Pisa University. His research interests centre on nonlinear dynamics and fluctuation theory and their application to a wide variety of problems, including tunneling of Bose-Einstein condensates in optical lattices, the nonlinear Wannier-Stark problem and the stock market.

References

[1] G. M. Zaslavsky, R. Z. Sagdeev, D. A. Usikov, and A. A. Chernikov, *Weak Chaos and Quasi-Regular Patterns*, Cambridge University Press (1991).

[2] W. K. Hensinger, H. Haffer, A. Browaeys, N. R. Heckenberg, K. Helmerson, C. McKenzie, G. J. Milburn, W. D. Phillips, S. L. Rolston, H. Rubinsztein-Dunlop, and B. Upcroft, *Dynamical tunnelling of ultracold atoms*, Nature 412 (6842), (2001), 52–55.

[3] D. A. Steck, W. H. Oskay, and M. G. Raizen, *Observation of chaos-assisted tunneling between islands of stability*, Science 293 (5528), (2001), 274–278.

[4] R. R. Scott, S. Bujkiewicz, T. M. Fromhold, P. B. Wilkinson, and F. W. Sheard, *Effects of chaotic energy-band transport on the quantized states of ultracold sodium atoms in an optical lattice with a tilted harmonic trap*, Phys. Rev. A 66 (2), (2002), 023407.

[5] T. M. Fromhold, A. A. Krokhin, C. R. Tench, S. Bujkiewicz, P. B. Wilkinson, F. W. Sheard, and L. Eaves, *Effects of stochastic webs on chaotic electron transport in semiconductor superlattices*, Phys. Rev. Lett. 87 (4), (2001), 046803.

[6] T. M. Fromhold, A. Patanè, S. Bujkiewicz, P. B. Wilkinson, D. Fowler, D. Sherwood, S. P. Stapleton, A. A. Krokhin,

L. Eaves, M. Henini, N. S. Sankeshwar, and F. W. Sheard, *Chaotic electron diffusion through stochastic webs enhances current flow in superlattices*, Nature 428 (6984), (2004), 726–730.

[7] D. Fowler, D. P. A. Hardwick, A. Patanè, M. T. Greenaway, A. G. Balanov, T. M. Fromhold, L. Eaves, M. Henini, N. Kozlova, J. Freudenberger, and N. Mori, *Magnetic-field-induced miniband conduction in semiconductor superlattices*, Phys. Rev. B. 76, (2007), 245303.

[8] A. G. Balanov, D. Fowler, A. Patanè, L. Eaves, and T. M. Fromhold, *Bifurcations and chaos in semiconductor superlattices with a tilted magnetic field*, Phys. Rev. E. 77, (2008), 026209.

[9] M. Kuraguchi, E. Ohmichi, T. Osada, and Y. Shiraki, *Relationship between Stark-cyclotron resonance and angular dependent magnetoresistance oscillations*, Physica E 12, (2002), 264.

[10] M. T. Greenaway, A. G. Balanov, E. Schöll, and T. M. Fromhold, *Controlling charge domain dynamics in superlattices by chaos-assisted miniband transport*, arXiv:0905.3717 .

[11] T. Hyart, J. Mattas, and K. N. Alekseev, *Model of the influence of an external magnetic field on the gain of terahertz radiation from semiconductor superlattices*, Phys. Rev. Lett. 103 (11), (2009), 117401.

[12] J. Touma and S. Tremaine, *A map for eccentric orbits in non-axisymmetric potentials*, Monthly Notices of Roy. Astron. Soc. 292 (4), (1997), 905–919.

[13] A. J. Lichtenberg and B. P. Wood, *Diffusion through a stochastic web*, Phys. Rev. A 39 (4), (1989), 2153–2159.

[14] W. Afanasiev, A. A. Chernikov, R. Z. Sagdeev, and G. M. Zaslavsky, *The width of the stochastic web and particle diffusion along the web*, Phys. Lett. A 144 (4-5), (1990), 229–236.

[15] V. I. Arnold, V. V. Kozlov, and A. I. Neishtadt, *Mathematical Aspects Of Classical And Celestical Mechanics*, Springer, Berlin (2006).

[16] A. J. Lichtenberg and M. A. Lieberman, *Regular and Stochastic Motion.*, Springer, New York (1992).

[17] G. M. Zaslavsky, *Physics of Chaos in Hamiltonian systems*, Imperial Colledge Press, London (2007).

[18] V. G. Gelfreich and V. F. Lazutkin, *Splitting of separatrices: perturbation theory and exponential smallness*, Russian Math. Surveys 56 (3), (2001), 499–588.

[19] G. N. Piftankin and D. V. Treshchev, *Separatrix maps in Hamiltonian systems*, Russian Math. Surveys 62 (2), (2007), 219–322.

[20] S. M. Soskin and R. Mannella, *Maximal width of the separatrix chaotic layer,* submitted to Phys. Rev. E.

[21] S. M. Soskin, R. Mannella, O. M. Yevtushenko, I. A. Khovanov, and P. V. E. McClintock, *A new approach to the treatment of separatrix chaos and its applications*, in A. Luo, ed., *Hamiltonian Chaos Beyond the KAM Theory* (dedicated to George Zaslavsky) arXiv:0906.3444v1, HEP-Springer, Berlin, pp. 000–000 (2009).

[22] G. Haller, *Chaos Near Resonance*, Springer-Verlag, New York (1999).

[23] M. Tabor, *Chaos and Integrability in Non-Linear Dynamics. An Introduction*, Wiley, New York (1987).

[24] B. V. Chirikov, *Resonance processes in magnetic traps* (in Russian), Atomnaya Energiya 6, (1959), 630–638.

[25] V. I. Arnold, *Instability of dynamical systems with many degrees of freedom*, Sov. Math. Dokl. 5, (1964), 581–585.

[26] G. M. Zaslavsky and M. Edelman, *Stochastic web as a generator of three-dimensional quasicrystal symmetry*, Chaos 17 (2), (2007), 023127.

[27] A. A. Chernikov, M. Y. Natenzon, B. A. Petrovichev, R. Z. Sagdeev, and G. M. Zazlavsky, *Some peculiarities of stochastic layer and stochastic web formation*, Phys. Lett. A 122 (1), (1987), 39–46.

[28] M. Abramowitz and I. Stegun, *Handbook of Mathematical Functions*, Dover, New York (1970).

[29] A. A. Chernikov, M. Y. Natenzon, B. A. Petrovichev, R. Z. Sagdeev, and G. M. Zazlavsky, *Strong changing of adiabatic invariants, KAM-tori and web-tori*, Phys. Lett. A 129 (7), (1988), 377–380.

[30] A. A. Chernikov, R. Z. Sagdeev, D. A. Usikov, M. Y. Zakharov, and G. M. Zazlavsky, *Minimal chaos and stochastic webs*, Nature 326, (1987), 559–563.

[31] S. M. Soskin, I. A. Khovanov, R. Mannella, and P. V. E. McClintock, *Enlargement of a low-dimensional stochastic web*, in M. Macucci and G. Basso, eds., *Noise and Fluctuations: 20th International Conference on Noise and Fluctuations (ICNF-2009)*, AIP, Melville, New York, vol. 1129, pp. 17–20 (2009).

[32] S. M. Soskin, I. A. Khovanov, R. Mannella, and P. V. E. McClintock, in preparation (2009).

[33] N. N. Bogolyubov and Y. A. Mitropol'sky, *Asymptotic Methods in the Theory of Nonlinear Oscillations*, Gordon and Breach, New York (1961).

[34] S. M. Soskin, R. Mannella, and O. M. Yevtushenko, *Matching of separatrix map and resonant dynamics, with application to global chaos onset between separatrices*, Phys. Rev. E 77 (3), (2008), 036221.

[35] Y. A. Kosevich, A. B. Hummel, H. G. Roskos, and K. Köhler, *Ultrafast Fiske effect in semiconductor superlattices*, Phys. Rev. Lett. 96, (2006), 137403.